

1
2
3 **Logging and lithostratigraphic study of the Cenomanian-Santonian**
4 **reservoirs of four oil wells MSP1, MSP2, MSP3 and MSP4 of the margin of**
5 **San-Pedro (Côte d'Ivoire)**
6
7

8 **ABSTRACT**

9 The logging and petrophysical study of four oil wells, MSP1, MSP2, MSP3 and MSP4 from
10 San-Pedro margin of the Ivorian sedimentary basin has made it possible to evaluate the
11 reservoir characteristics of the Cenomanian-Santonian age formations. Lithostratigraphically,
12 this study has shown that this interval consists of clay and sandstone deposits interspersed
13 with frequent past carbonate.

14 At the logging, ten (10) sandstone reservoirs are highlighted with effective porosities ranging
15 from 16% to 21% and permeabilities from 100 mD to 1100 mD (millidarcy).

16 These reservoirs have very good petrophysical characteristics however their high water
17 saturation show that they are rather aquifers. The various log gamma ray profiles of the
18 intervals considered highlight a fluvial and marine deposition environment. Sedimentation
19 would have started in a Cenomanian-type fluvial environment and would have continued in a
20 marine environment marked by the accumulation of sandstone and clay under the influence of
21 transgression and regression phases in the Turonian and Lower Senonian.

22
23
24 **Keywords :** *Logging; Reservoirs; lithostratigraphy; petrophysics; Ivorian basin;*
Cenomanian; Santonian; depositing environment
25

26 **1. INTRODUCTION**

27 Located in the southern part of the country, the Ivorian sedimentary basin grows along the
28 West Atlantic coast from Liberia (Sassandra) to Ghana. It extends between 3 ° 05 W and 7 °
29 30 W and develops south of the latitude 5 ° 20 N. It results from the opening of the South
30 Atlantic to the Jurassic and is part of the chain of sedimentary basins bordering the west
31 Atlantic coast from southern Morocco to southern Africa [1].

32 This basin is of Meso-Cenozoic age [2] and includes a terrestrial part (onshore) or coastal
33 basin and a submerged part (offshore) object of this study.

34 The submerged basin or offshore basin represents the largest part of the basin and develops on
35 the continental shelf area, 750 km wide [3]. This offshore basin is studied only by oil drilling.

36 It presents a structure in horsts and grabens, in response to the action of transtension
37 phenomena that surround it. These are the transforming faults of Saint-Paul in the North-West
38 and Romanche in the South-East [4, 5, 6].

39 This offshore basin is subdivided into a margin of Abidjan and a margin of San Pedro.

40 The Abidjan margin is the area of the main hydrocarbon discoveries in Côte d'Ivoire. It
41 contains all the oil fields (Baobab, Lion, Hope, Foxtrot ...) known to date.

42 The oil exploration campaigns conducted so far at the San Pedro margin have not yet revealed
43 sufficient commercial hydrocarbon accumulations to justify exploitation.

44 These less favorable oil results from recent wells drilled in this western part of the
45 sedimentary basin of Côte d'Ivoire are prompting new geological studies to better understand
46 the oil system of this margin. It is in this context that this study is initiated.

47 The main objective sought in this study is to characterize the Cenomanian-Santonian
48 reservoirs of this zone at logging and lithostratigraphic and petrophysical levels. The choice
49 of this interval obeys the fact that most deposits in the Abidjan margin have ages in this range.
50 This study also aims to identify the reservoir zones from their lithological and petrophysical
51 characteristic

52
53

54 2. PRESENTATION OF THE STUDY AREA

55 The study area is located in the Ivorian offshore sedimentary basin. This basin covers an area
56 of about 22000 km² and a width of 80 km to 150 km from east to west from the coast to
57 depths of water above 3000 m. It constitutes the bulk of the Ivorian sedimentary basin. It
58 presents a structure in horsts and grabens, in response to the action of transtension phenomena
59 that surround it.

60 These are the transforming faults of Saint-Paul in the North-West and Romanche in the
61 South-East [4, 5, 6]. This deep basin is subdivided into a margin of San-Pedro in the west and
62 a margin of Abidjan in the east which are two geologically distinct margins (Fig. 1):

63

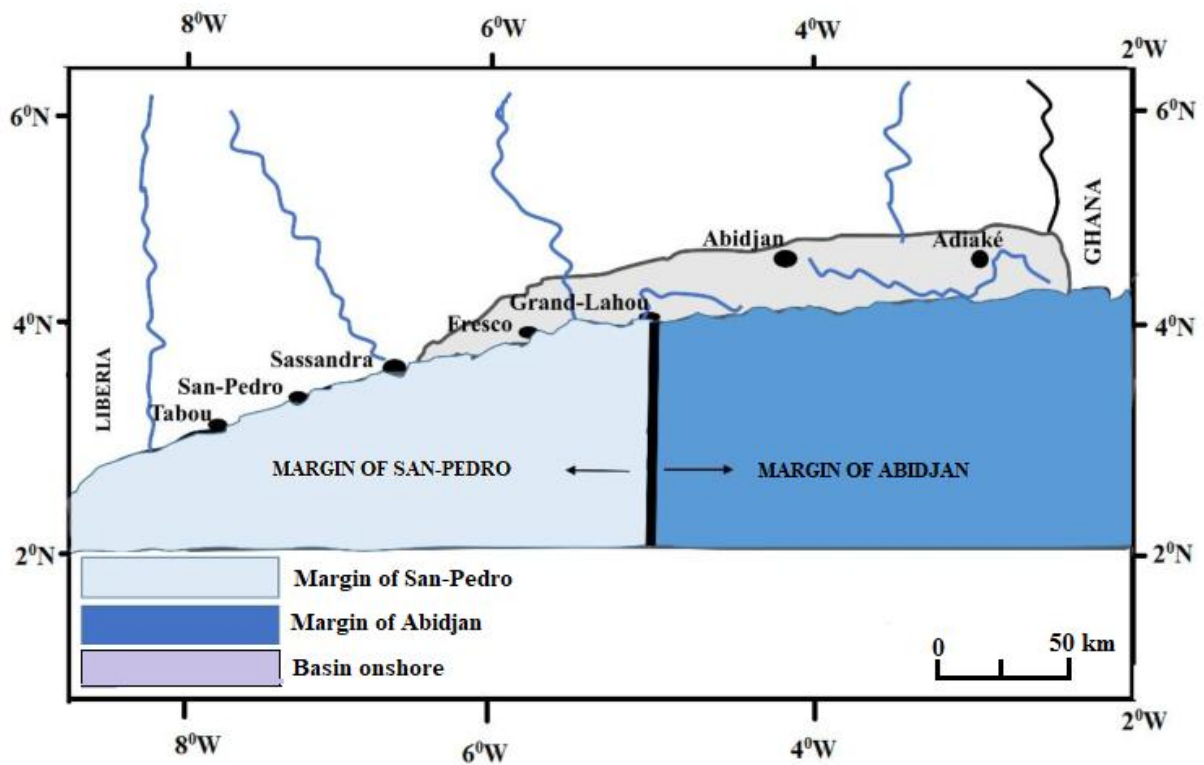
64 - The margin of San-Pedro extends from the Liberian border to the city of Grand-Lahou. This
65 margin is characterized by a deep basement, about 8 km according to the magnetic data of [7].
66 This Socle on which is located a steep continental shelf characteristic of the West margin, is
67 part of the offshore extension of the West African craton. The sediments thicken from north to
68 south where they reach about 700 to 800m at the top of the slope.

69

70 - The margin of Abidjan extends from Grand-Lahou to the Ghanaian border. This margin is
71 characterized by a deep basement where sediment thickness increases from west to east
72 (towards the Ghanaian basin) [8].

73 This thickness was estimated by [7] between 6 and 10 Km by magnetic methods, but the
74 seismic overestimated it between 12 and 13 Km. South of Abidjan, the plateau is cut by the
75 bottom hole.

76



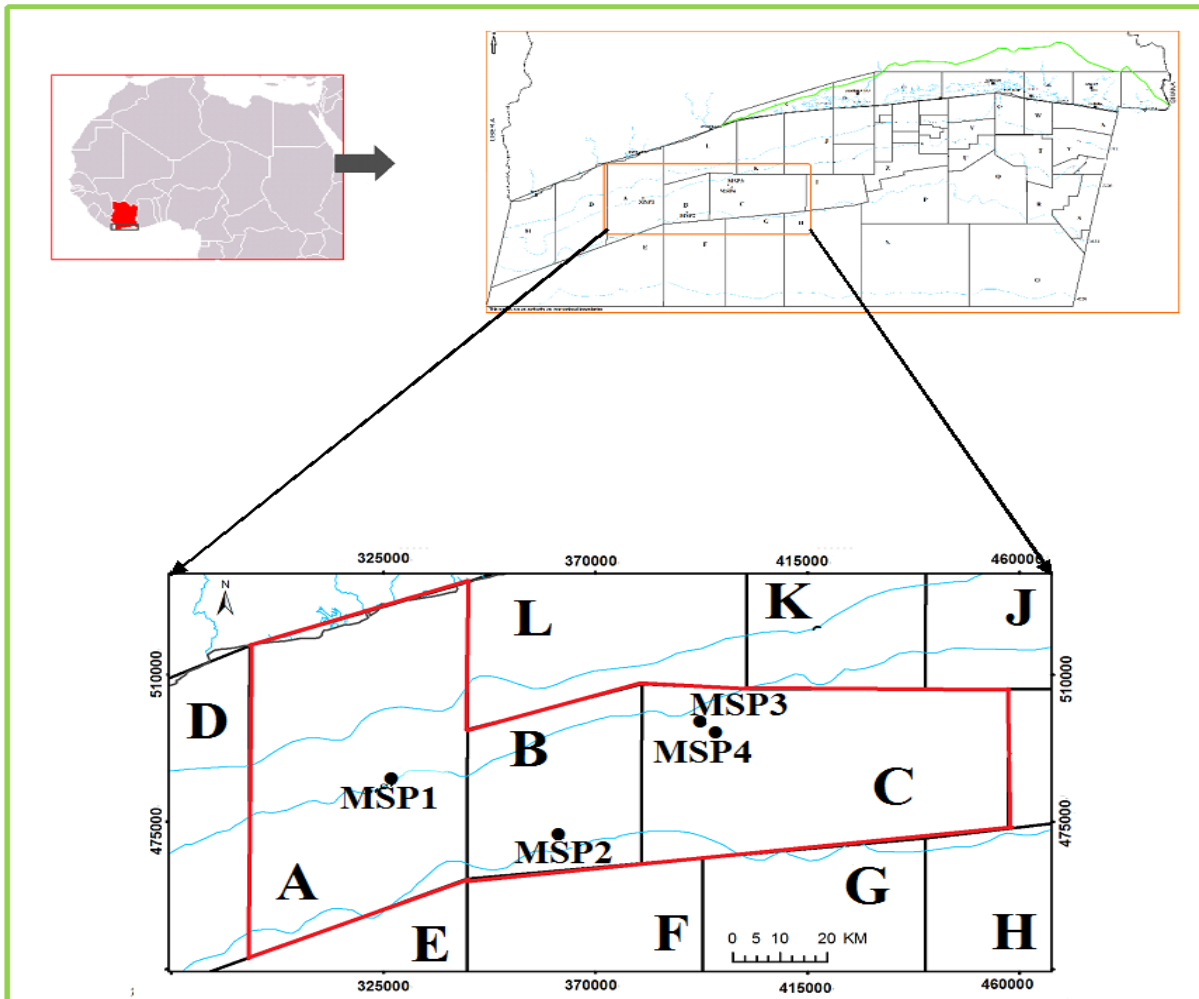
77
78
79
80
81
82
83
84
85

Fig. 1. Margins of the sedimentary basin of Côte d'Ivoire

The whole Ivorian sedimentary basin is divided into forty-eight (48) petroleum blocks today. This study area has fifteen (15) and nine (9) exploratory wells of which four (4) are studied in this work. These wells are located in blocks A, B and C of the San-Pedro Margin (Fig. 2). The coordinates of these wells are shown in Table 1 below.

Table 1. Wells coordinates

Block	Wells	Latitude	Longitude	Depth (m)
A	MSP-1	4°23'27,9098''N	6°34'02,2528''W	1838,5
B	MSP-2	4°16'29,841'' N	6°14'43,912'' W	2864
C	MSP-3	4°30'58,249'' N	5°57'31,953'' W	2162
	MSP4	4° 29' 51,756'' N	5°56'44,100'' W	2303



86

87 **Fig. 2. Location of the wells**

88

89 **3. MATERIALS AND METHODS**

90

91 The material **used of this** work consists of technical data **of** drilling reports, digital logging
 92 data (L.A.S files), composite logs and computer equipment.

93 L.A.S (Log Ascii Standard) files are digital files that contain the log data from records made
 94 during Wireline or LWD operation.

95 **Drilling** reports provide information on the lithology and petrophysical properties of the **rock**
 96 layers traversed by the different wells studied.

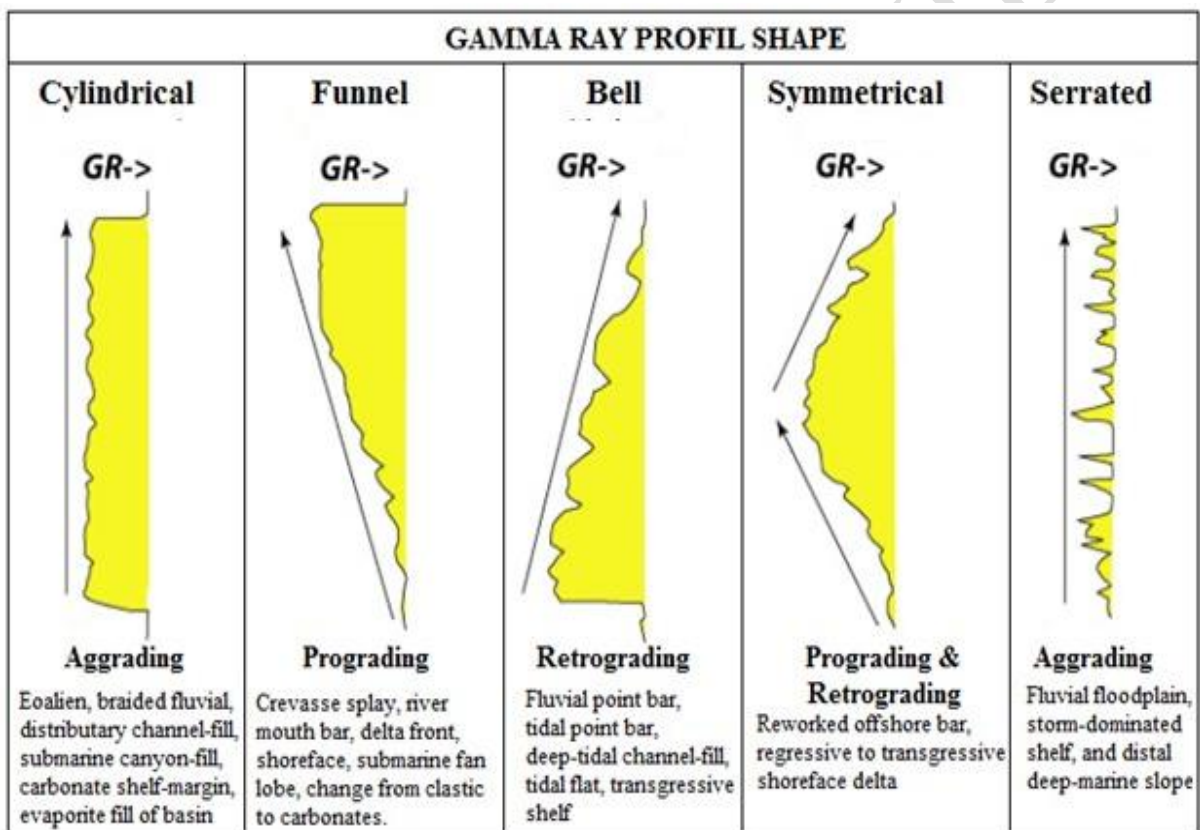
97 Composite logs are a set of logging signatures consisting of Gamma ray, Sonic, Resistivity,
 98 Density and Neutron logs derived from digital logging data.

99 Computer hardware is made up of high-capacity computers and software, the Decision Space
 100 Geosciences (DSG) software. It is a multifunction software, which has applications in
 101 geology, geophysics and petrophysics. It allows, log analysis, loading, processing and logging
 102 data interpretation.

103 The methodological approach used is based exclusively on log analysis and interpretation.

104 Logging digital data recorded in L.A.S (Log Ascii Standard) format during acquisition is
 105 loaded into a database and processed using Decision Space Geosciences (DSG) software.

106 Once the files, we proceed to the assignment of the curves, the positioning of the roofs of the
 107 floors and the development of the lithological logs.
 108 The assignment consists of matching the curves to each type of log (Gamma Ray, Sonic,
 109 Resistivity, Density and Neutron).
 110 Once log logs have been constructed, the different lithological formations the borehole are
 111 characterized, on the basis of the signatures of the gamma ray and density-neutron logs and
 112 verified by the drill cuttings descriptions and the biostratigraphic analysis.
 113 The potential reservoir zones correspond to the low values of gamma ray and whose thickness
 114 is greater than or equal to 10m.
 115 The gamma ray profile analysis also makes it possible to define the depositional
 116 environments. This analysis is based on the comparison shape of the gamma ray profile with
 117 the standard model (Fig. 3) established by [9].
 118 The petrophysical characterization of potential reservoirs, to determine : porosity (Φ),
 119 permeability (K), clay volume (Vsh), water saturation (Sw) and Net / Gross (N / G).
 120



121
 122 **Fig. 3. Standard gamma ray (GR) response model based on variation in grain size and**
 123 **deposit environments [9]**

124
 125 These parameters are calculated from formulas integrating log data. These formulas having
 126 been automated, they are directly processed by computer from specialized software such as
 127 Techlog.
 128
 129
 130
 131
 132

133 ➤ **Effective porosity (Φ_e)**

134 It excludes unconnected pores and clay-bound water [10]. His formula is as follows:

135 $\Phi_e = \Phi_t \times (1 - V_{sh})$ with V_{sh} (volume of clay) Eq.1

136

137 There are three types of reservoir according to their porosity (Φ_e) :

- 138 - low porosity reservoir : (Φ_e) < 5% ;
- 139 - medium porosity reservoir : 10% < (Φ_e) < 20% ;
- 140 - good porosity reservoir : (Φ_e) > 20%.

141

142 ➤ **Permeability (K)**

143 The empirical formula of [11] based on the irreducible saturation method was used to assess the permeability.

145 $K = (0,136 \times \Phi_e^{4,4}) / (S_w)_{irr}^2$ Eq.2

146 With :

- 147 **K** : permeability millidarcy ;
- 148 $(S_w)_{irr}$: irreducible water saturation in percentage ;
- 149 Φ_e : effective porosity in percentage

150

151 ➤ **Volume of clay (V_{sh})**

152 The volume of clay is calculated from the density-neutron logs and checked with gamma ray according to the formula:

153

155 $V_{sh} = [GR_{luc} - GR_{min}] / [GR_{max} - GR_{min}]$ Eq.3

156

157 • **GR_{luc}** : GR value of the given bench read directly from the log (API) ;

158 • **GR_{min}** : minimum GR value of the same bench (API) ;

159 • **GR_{max}** : maximum GR value of the same bench (API).

160

161 ➤ **Water saturation (S_w)**

162 The water saturation is calculated using the equation of [12]:

163 $S_w = ([a \times R_w] / [R_t \times \Phi_t^m])^{1/n}$ Eq.4

164 With:

- 165 **S_w** : water saturation ;
- 166 **a** : Archie tortuosity factor;
- 167 **R_w** : resistivity of formation water ;
- 168 **R_t** : resistivity of deep formation ;
- 169 **Φ_t** : total porosity ;
- 170 **m** = Archie's cementing exponent;
- 171 **n** = saturation exponent of Archie.

172

173 ➤ **Net/Gross (N/G)**

174 This is a parameter that provides information on the quality of the reservoir. This is the Net ratio (ie the net thickness of sand) on the Gross (which corresponds to the total thickness of the reservoir).

177 So depending on the percentage obtained, the reservoir will be classified as:

- 178 - poor quality N / G < 0.1 ;
- 179 - medium quality 0.1 < N / G < 0.5;
- 180 - very good quality N / G = 1.

181 These parameters are interpreted in general by the cut-off below proposed by [13]. According to him, a good rock reservoir is one that meets the characteristics below.

182

- 183 - Porosity (Φ) > 10%
- 184 - Volume of clay (Vsh) < 40%
- 185 - Water saturation (S_w) < 60%
- 186 - Net / Gross > 20%

189 4. RESULTS

191 4.1 Identification of top and potential reservoirs

192 The log signatures analysis coupled with the biostratigraphy data allowed to identify the top
193 of the different formation of the studied wells. The results are shown in Table 2 below.

194 It is noted that the layers are thicker in wells further south such as MSP-2 and MSP-4 than
195 those located in the north (MSP-1 and MSP-3). Sediment thickness increases from north to
196 south.

197 **Table 2. Top of the formation of studied wells**

Wells	MSP-1	MSP-2	MSP-3	MSP-4
Top of stage (m)				
Top of Santonian	2960	5068	3821	3976
Top of Coniacian	Eroded	Eroded	3878	4098
Top of Turonian	3080	5162.5	3980	4219
Top of Cénomaniian	3260	5370	4090	4315
Cenomanian base	3430	Not reached	4228	4529

198
199 These stages are confirmed by recent biostratigraphy data. Recent palynological data
200 distinguish a Lower Cenomanian characterized by the presence of pollen species
201 *Triporopollenites* sp.; *Classopolis echinatus*, *Classopolis spinosus*, *Afropollis gardenus* and
202 *Steevesipollenites binodosus*.

203 As for the Upper Cenomanian, it is characterized by the association composed of spores and
204 pollen *Classopolis echinatus*, *Afropollis jardinus*, *Steevesipollenites binodosus*, *Triorites*
205 *africaensis*, *Classopollis* sp., *Pemphixipollenites inequixinus*, *Galeocornea causea*,
206 *Ephedripites* sp., *Gnetaceapollenites diversus*, *Classopollis classoides* (Plate 1).

207
208 The microfauna is dominated by the planktonic foraminifera *Herdbergella planispira*,
209 *Herdbergella delrioensis*, *Herdbergella* sp. and *Globigerinoides bentonensis* [14].

211 ➤ Turonian

212 The highlight of Turonian is mainly planktonic foraminifera: *Whiteinella baltica*, *Whiteinella*
213 *paradubia* *Herdbergella delrioensis*, *Herdbergella simplex*, *Heterohelix moremani*,
214 *Whiteinella archaeocretacea* [15, 16].

215 Palynologically, no species has been clearly described as a good stratigraphic marker.
216 However, Turonian is characterized from pollen grains *Florentinia radiculata*, *Florentinia*
217 sp., *Tricolpites giganteus*, *Odontochitina operculata*, *Tricolpites* sp., *Tricolpites*
218 *microstriatus*, *Tricolpites* sp., and *Parasyncolpites* sp. [15] (Plate 2).

219
220
221
222
223
224
225
226
227
228
229
230
231
232
233
234
235
236
237
238
239
240
241
242
243
244
245
246
247
248
249
250
251
252
253
254
255
256
257
258
259
260

➤ **Lower Senonian (Santonian-Coniacian)**

The lower Senonian is characterized by the planktonic foraminifera *Dicarinella concavata*, *Marginotruncana renzi*, *Hastigerinoides alexanderi*, *Herdbergella sp.* and *Heterohelix globulosa* [17].

Palynologically, this stage is characterized by marker dinocysts such as *Canningia sp.*, *Oligosphaeridium complex*, *Dinogymnium acuminatum*, *Dinogymnium sp.*, *Xenascus sp.*, *Oligosphaeridium pulcherrinum*, *Circulodinium distinctum*, *Droseridites senonicus*, and *Ariadnaesporites spinosus* [18] (Plate 3).

4.2 Reservoirs oil potentials

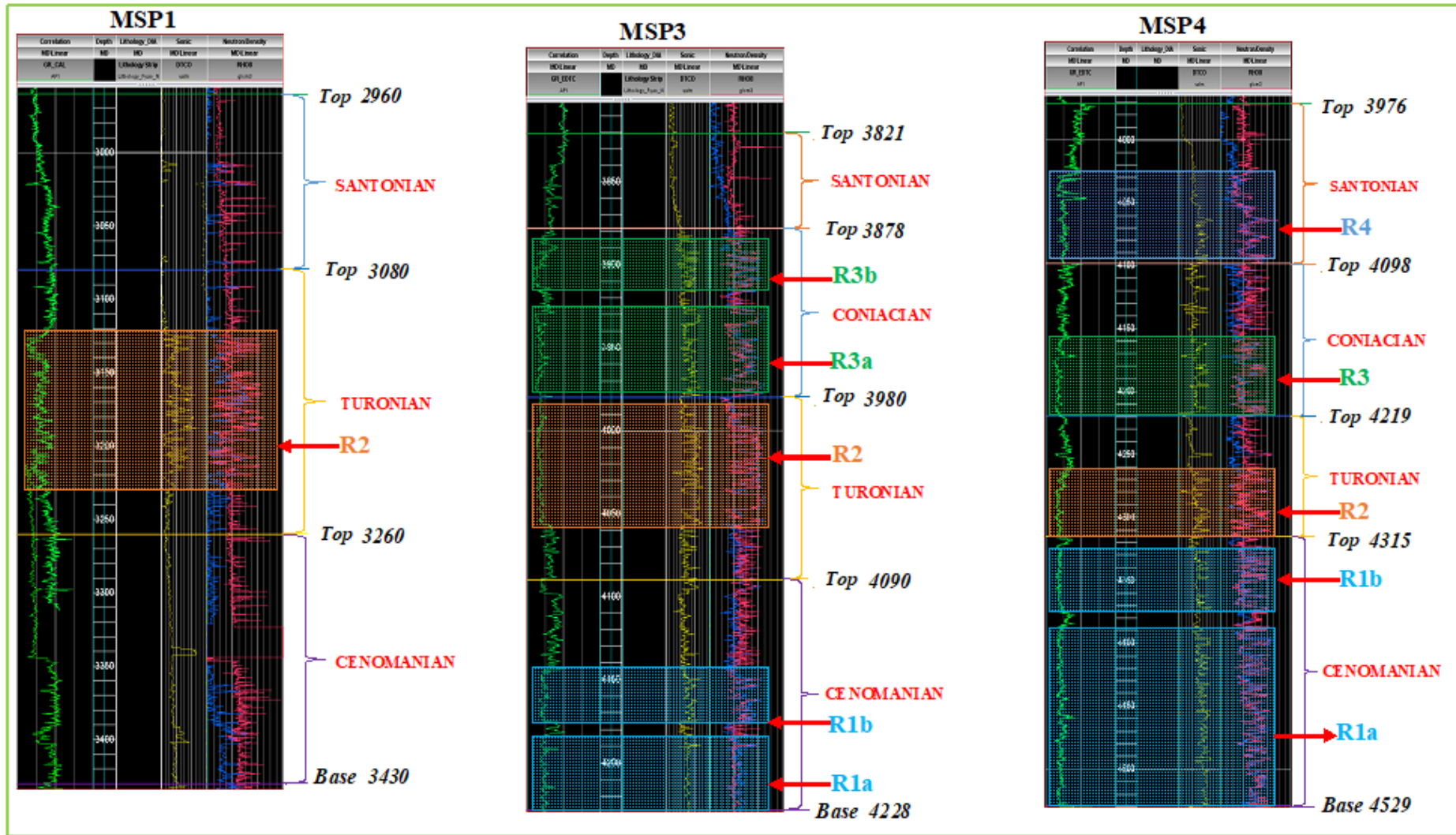
Analysis of Gamma Ray (GR) data from the wells revealed potential reservoirs. Classically, gamma-ray is used for the determination of clay and sand formations. The highest values of gamma ray correspond to the clay formations and the lowest values to the sandy formations.

In principle, gamma ray measures the clayiness of the formation [19]. This study revealed ten (10) reservoir levels of variable thickness in the four wells studied. Table 3 below gives details of these reservoirs and their lithostratigraphic characteristics. Some reservoirs have small discontinuity intervals which are in fact clay beds of high gamma Ray value interspersed in a zone of low values (Fig. 4 and 5). These intercalations are encountered in the tanks R3 and R1 compartmentalized in tanks R3a, R3b and in tanks R1a and R1b at the wells MSP-3 and MSP-4.

The reservoir levels encountered in this study mainly consist of calcareous, clay and sandstone. These reservoirs are clay and silts. They are covered by thick layers of clay or silts (Fig. 6).

Table 3. Potential reservoirs and their lithostratigraphic characteristics

Reservoirs of stage	Wells			
	MSP-1	MSP-2	MSP-3	MSP-4
Santonian (R4)	No reservoir R4	R4 (95m) Sandstone white to gray with fine to very coarse grains	No reservoir	R4 (70m) Fine to coarse sandstone poorly cemented with a clay-limestone cement
Coniacian (R3)	No reservoir R3	No reservoir R3	R3b (50m) Fine to coarse sandstone, compacted or not, with limestone cement	R3 (50,5m) Very fine to medium sandstone with limestone cement,
			R3a (60m) Fine to coarse sandstone, compacted or not, with limestone cement	
Turonian (R2)	R2 (110m) Coarse sandstone, with limestone cement	R2 (90m) Gray sandstone, fine to medium, with limestone cement and clay interlayers	R2 (70m) Fine to coarse sandstone with limestone cement	R2 (55m) Gray sandstone, very fine to medium, with limestone cement
Cenomanian (R1)	No reservoir R1	No reservoir R1	R1b (23m) Fine to coarse sandstone, compacted or not, white to gray, calcareous cement	R1b (54m) Very thin to medium gray to light gray to calcareous cement
			R1a (38m) Fine to coarse sandstone, compacted or not, white to gray, calcareous cement	R1a (146m) Very thin to medium gray to light gray to calcareous cement



264
265

AA

266

Fig. 4. Potential reservoir levels of MSP1, MSP3 and MSP4 wells

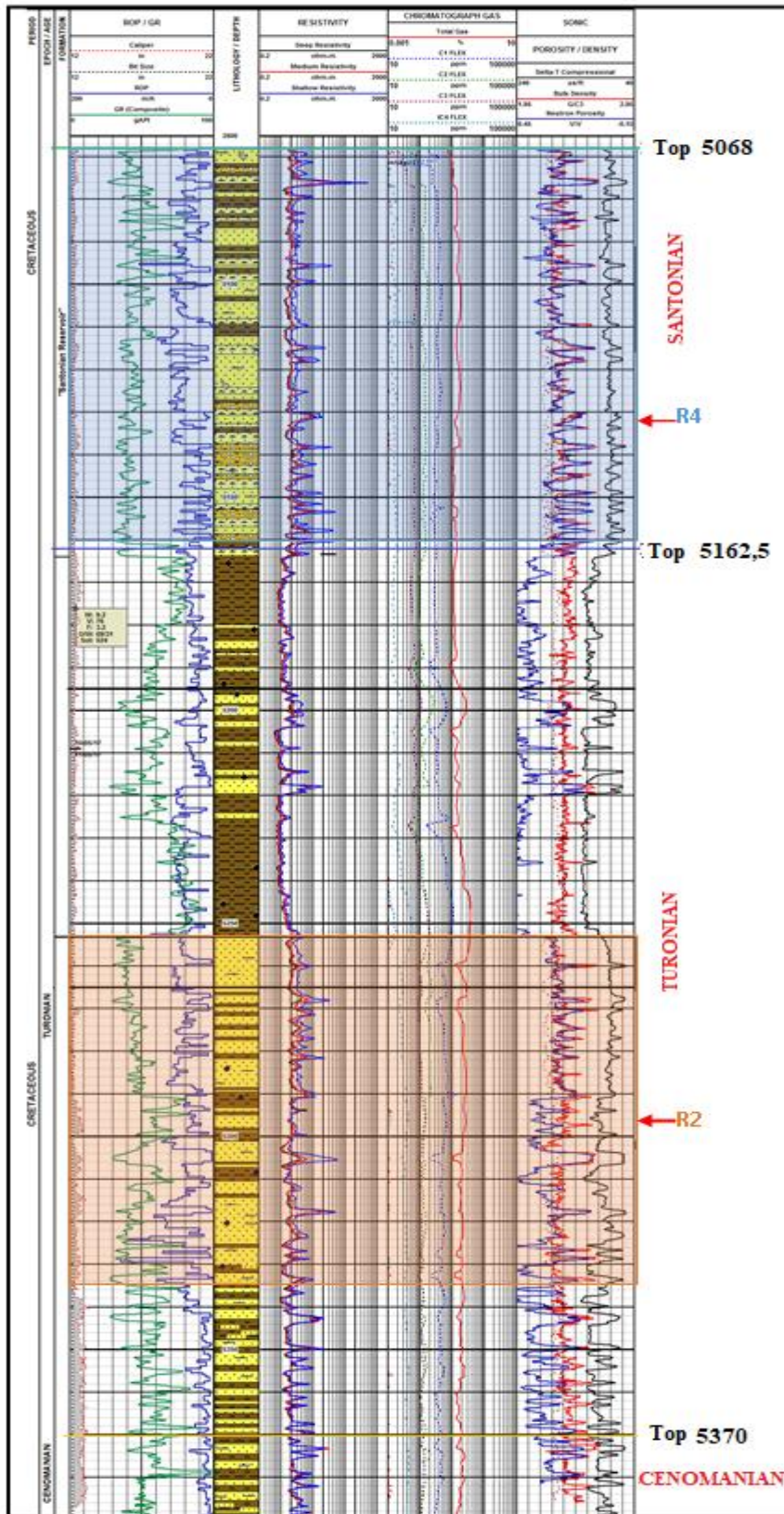
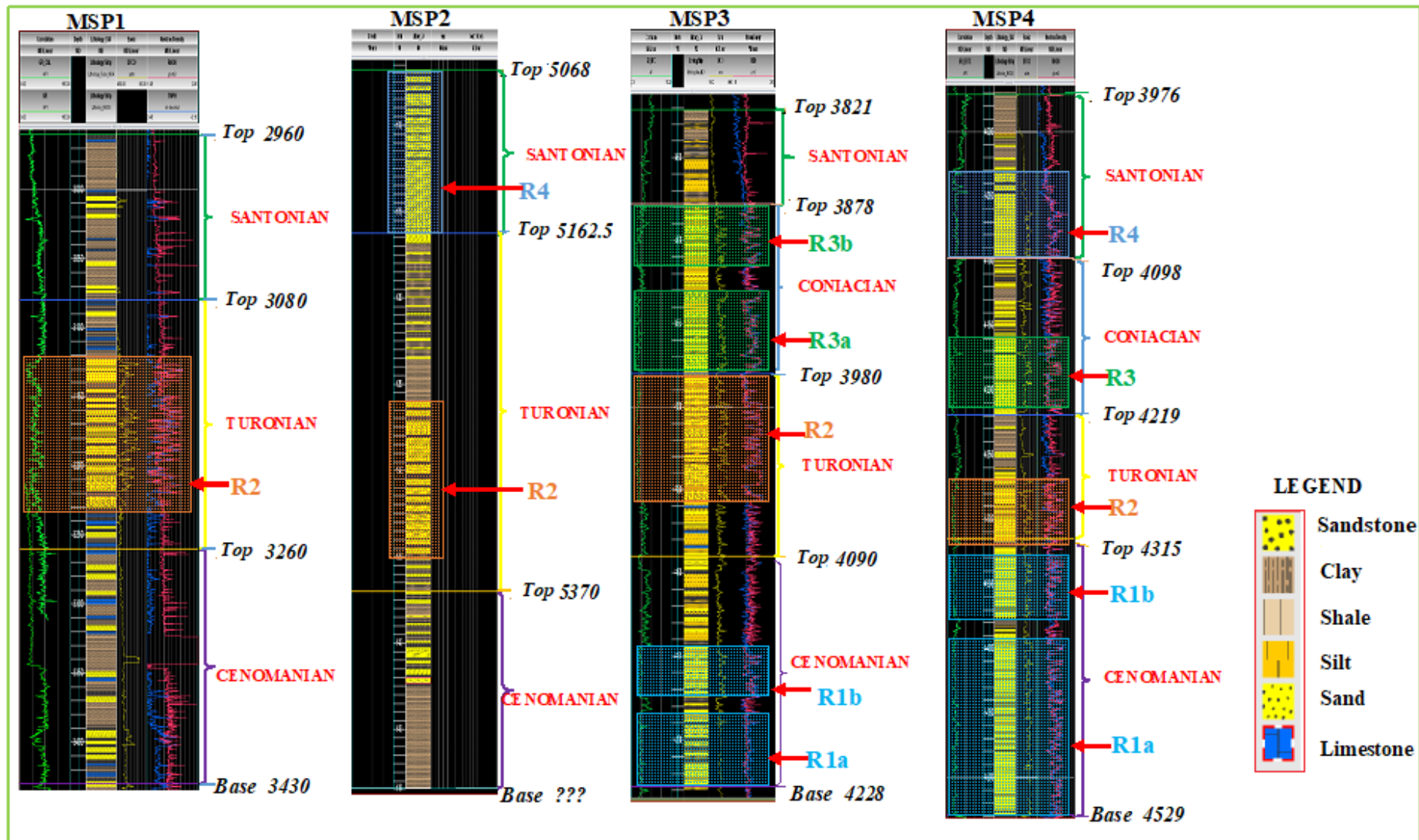


Fig. 5. Potential reservoir levels of the MSP2 well

267
268
269



270

271 Fig. 6. Lithostratigraphic log of the different wells studied

272 **4.3 Correlation of reservoir levels of studied wells**

273 The West-East correlation profile between the different reservoirs (**Fig. 7**) shows that only the
 274 turonian reservoir (R2) is continuous over the entire profile and that its thickness decreases
 275 progressively from west to east. As for the other tanks, they are discontinuous. The
 276 Cenomanian (R1) and Coniacian (R3) reservoirs are present only in the East. We also note
 277 that the Santonian reservoir (R4) is absent in the center of the profile that is to say in the block
 278 B and that its thickness decreases from West to East. This can be explained by erosion caused
 279 by eustatic variations in the Ivorian sedimentary basin. The absence of R1 and R3 in the rest
 280 of the zone may be due to a no deposit phase or erosion. If the thickness of the tank R3
 281 decreases towards the East, the thickness of R4 increases.
 282

283 **4.4 Petrophysical characteristics of reservoirs**

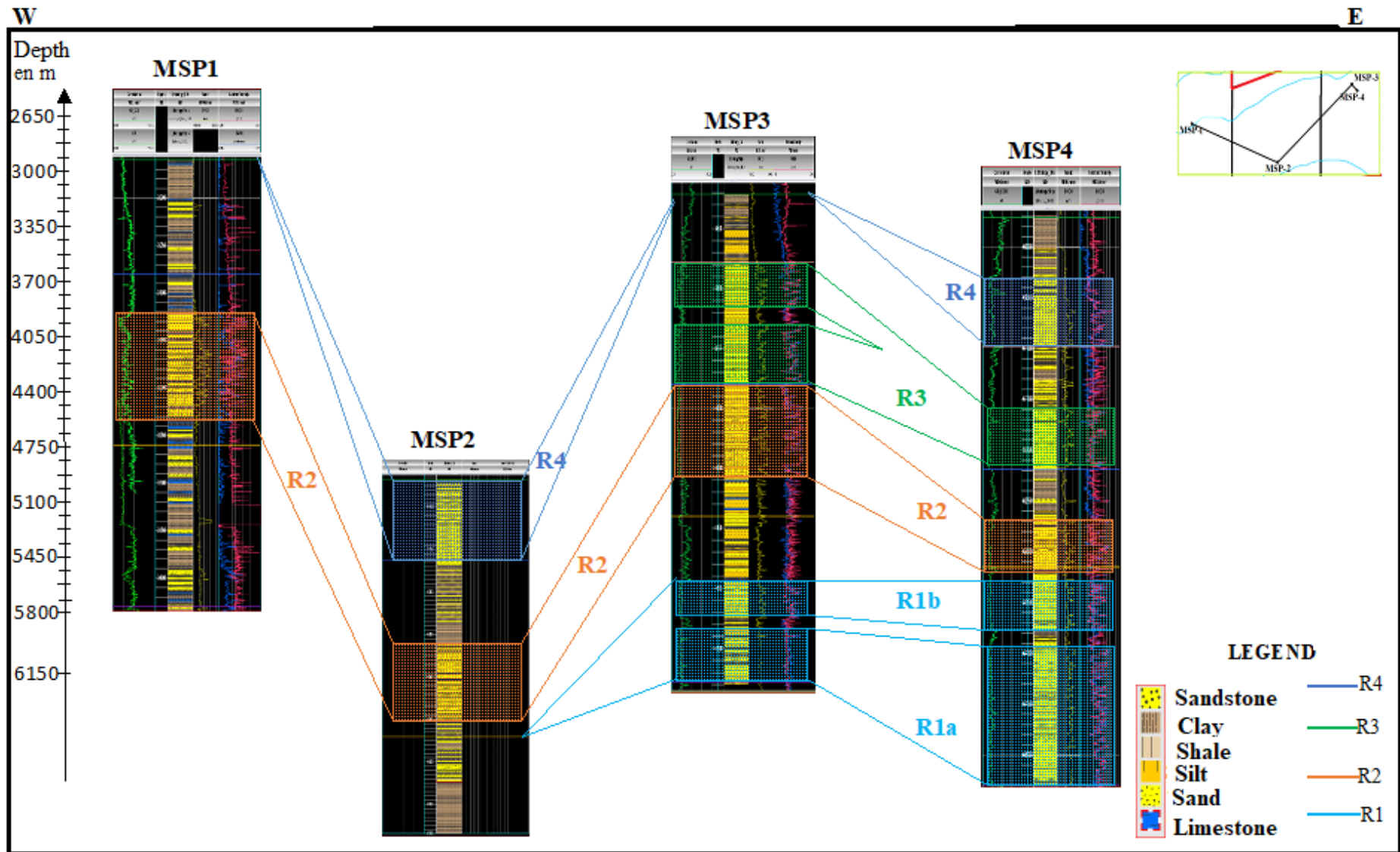
284 The results of the petrophysical evaluation are recorded in the table 4 below.
 285

286 **Table 4. Results of the petrophysical study**

BLOCK	WELLS	FORMATIONS	INTERVAL					RESERVOIRS					
			EXTENSION (m)	Gross (m)	GR (API)	Net (m)	N/G (%)	VSH (%)	PHIE (%)	PERM (mD)	SWE (%)	FLUID	
A	MSP1	TURONIAN	3120-3230	110	37	30	29	21	21	155	98	water	
B	MSP2	SANTONIAN	5068 - 5162.5	95	45-60	80	83	19	20.1	NA	100	water	
		TURONIAN	5260 - 5350	90	45-60	60	67	25	19.6	NA	99	water	
	MSP3	CONIACIAN	3878-3980	102	15-30	53	52	11	18	NA	94	water	
		TURONIAN	3980-4060	80	25-37	31	39	12	19	NA	86	water	
C	MSP3	CENOMANIAN	4153-4228	75	30-37	40	53	15	16	NA	95	water	
		SANTONIAN	4028-4098	70	30-45	46	66	13	18	100-1100	81	water	
	MSP4	CONIACIAN	4155-4219	64	25-30	56	88	14	18	100-300	94	water	
		TURONIAN	4260-4315	55	25-30	47	86	17	18	NA	95	water	
		CENOMANIAN	4315-4529	214	30-45	193	90	8	20	400-700	91	water	

287
 288 The analysis of the petrophysical parameters reveals generally for the different wells studied
 289 that:

- 290 ➤ Porosity (Φ) varies from 16% to 21% in all tanks. This result indicates that the
 291 reservoirs have medium to good porosities.



292

293

Fig. 7. West-East Correlation Profile of Well Wells Studied

- 294 ➤ **Volume of clay (Vsh):** With the exception of the reservoir R2 of the MSP2 well,
295 which can be qualified as a medium quality reservoir with a Vsh of 25%, the other
296 reservoirs are good qualities because the volume of clay is less than 20%.
297
- 298 ➤ **Water saturation (SW):** This study shows that the water saturation of the different
299 tanks is greater than 80%. This result indicates that the identified reservoirs are
300 aquifers.
301
- 302 ➤ **Net to Gross (N / G):** The Net to Cross values are above 20% and indicate that the
303 tanks are good qualities.
304

305 In general, [13] estimates that an oil reservoir is of good quality if the cut-off values of the
306 following parameters are respected:

- 307 - Porosity (Φ) > 10%
308 - Volume of clay (Vsh) < 40%
309 - Water saturation (Sw) < 60%
310 - Net / Gross > 20%

311
312 With the exception of water saturation, our results indicate that the potential reservoirs
313 highlighted are of good quality. They have all the necessary characteristics to store
314 hydrocarbons except that they are all aquifers.
315
316

317 **4.5 Deposit environments of reservoir levels**

318 From the different form of the Gamma Ray profile of the identified reservoir levels, the
319 associated depositing environments are determined. **Fig. 8, 9, 10 and 11** below indicate the
320 deposition environments of the identified reservoirs.

321 At the Cenomanian, reservoir sediments deposited either in a fluvial environment because of
322 the serrated form of the Gama Ray or marine with strong fluvial influence because of
323 cylindrical shape that tends towards the serrated form of Gama Ray (**Fig. 8**). This is
324 confirmed by the palynological data which indicates a predominance of spores and pollen
325 grains characteristic of a continental environment (**Plate 1**). Also the marine influence is
326 indicated by the presence of foraminifers.

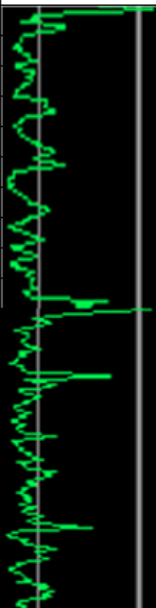
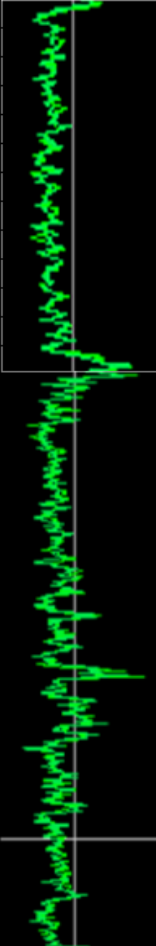
327
328 In Turonian, reservoir sediments were deposited in environments ranging from marine to
329 fluvial through deltaic environments due to the combination of cylindrical, serrated, funnel
330 and bell-shaped Gama Ray (**Fig. 9**). This is confirmed by the presence of dinocyst which
331 characterizes this marine environment (**Plate 2**).

332 At the Conancian and Santonian tanks were set up in a marine environment (**Fig. 10 and 11**).
333 This is confirmed by the presence of dinocyst which characterizes this marine environment
(**Plate 3**).

334
335 From this study, two dominant deposition environments emerge. Sedimentation would have
336 started in a fluvial environment and would have continued in a marine environment marked
337 by the accumulation of sandstone, clay, limestone. However, frequent variations of the
338 deposition conditions in connection with the phenomena of transgressions and regressions are
339 observed.
340

341

342

WELLS	STAGE	RESERVOIR	GAMA RAY	SHAPE	DEPOSIT ENVIRONMENT
MSP3	CENOMANIAN	R1b		CYLINDRICAL	MARINE DEPOSITION UNDER FLUVIAL INFLUENCE
		R1a		CYLINDRICAL	
MSP4	CENOMANIAN	R1b		CYLINDRICAL	MARINE DEPOSITION UNDER FLUVIAL INFLUENCE
		R1a		CYLINDRICAL	
					INDENTED

343

344

345

346

Fig. 8. Cenomanian reservoir deposit environments

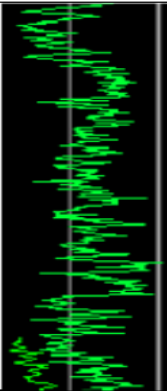
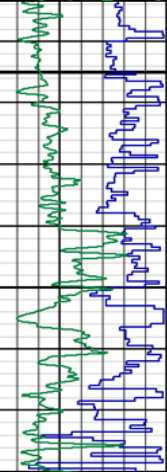
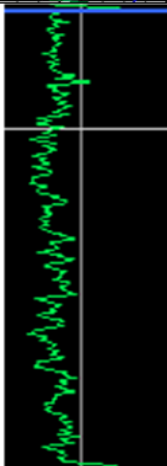
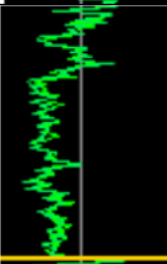
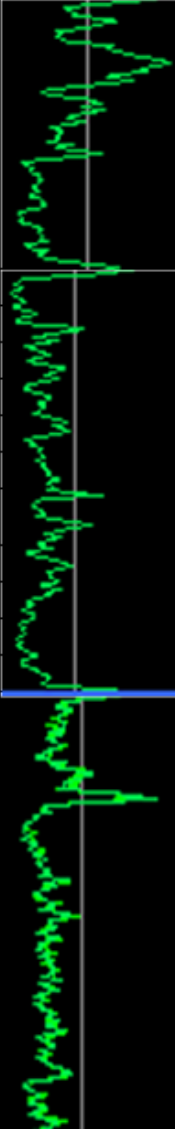
WELLS	STAGE	RESERVOIR	GAMA RAY	SHAPE	DEPOSIT ENVIRONMENT
MSP1	TURONIAN	R2		CYLINDRICAL	MARINE
				BELL	FLUVIAL
				INDENTED	
				FUNNEL	
MSP2	TURONIAN	R2		CYLINDRICAL	MARINE
				SYMMETRICAL	DELTAIC
				BELL	
MSP3	TURONIAN	R2		INDENTED	DELTAIC
MSP4	TURONIAN	R2		CYLINDRICAL	MARINE

Fig. 9. Turonian reservoir deposit environments

WELLS	STAGE	RESERVOIR	GAMA RAY	SHAPE	DEPOSIT ENVIRONMENT
MSP3	CONIACIAN	R3b		CYLINDRICAL	MARINE
		R3a		CYLINDRICAL	MARINE
				SYMMETRICAL	DELTA
MSP4	CONIACIAN	R3		CYLINDRICAL	SUBMARINE CHANNEL DEPOSIT
				CYLINDRICAL	

352
 353
 354
 355
 356

Fig. 10. Conancian reservoir deposit environments

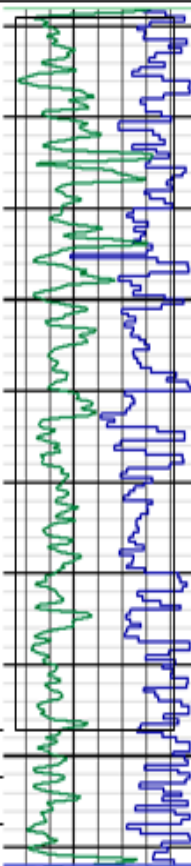
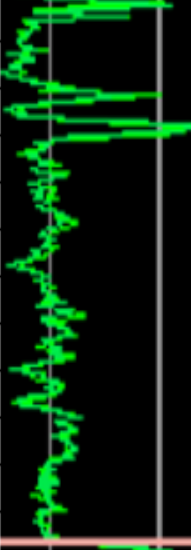
WELLS	STAGE	RESERVOIR	GAMA RAY	SHAPE	DEPOSIT ENVIRONMENT
MSP2	SANTONIAN	R4		CYLINDRICAL WITH INTERSPERSED CLAY LEVEL AT THE TOP	MARINE
MSP4	SANTONIAN	R4		CYLINDRICAL CYLINDRICAL	MARINE

Fig. 11. Santonian reservoir deposit environments

357
358
359
360
361

362 **5. DISCUSSION**

363 The identification of reservoir levels based on low gamma ray profiles was used by [20] in
364 Benin to highlight Albian reservoirs in the deep offshore part of the Beninese coastal basin.
365 These potential reservoirs are sandy with a variable percentage of clay that serves as cement.
366 Thus, with this method, 10 silty reservoir levels presenting clay levels by location are
367 highlighted and are consistent with those obtained by [21] which indicate that the reservoirs
368 of Côte d'Ivoire basin are sandstone.

369 **➤ Lithostratigraphy**

370
371
372 This study reveals that sedimentation is mainly silico-clastic dominated by clays and
373 sandstones (dominant facies) and incidentally silts, sands and limestones. [17] has shown that
374 deposits in the Upper Albian-Lower Senonian interval of the Ivorian sedimentary basin are
375 characterized by clay-sandstone deposits locally enriched with limestone. The results of
376 Chierici were confirmed by those of [2] and recalled by [22].

377 The gritty nature of the reservoirs described in this work is confirmed by the work of [21].
378 [7] demonstrated that the lithology of reservoir levels of the Abidjan margin in the
379 Cenomanian-Santonian interval is identical to that described in this study on the margin of
380 San-Pedro.

381 **➤ Correlation**

382
383 The correlation established between the reservoir levels shows that the thickness of the
384 Turonian reservoirs is gradually decreasing from west to east of our study area as described
385 by the results of [23] recalled by [22], which showed that the Turonian is not visible
386 throughout the basin because it is strongly eroded during the Turonian [17] or Senonian
387 regression [2].

388 The effect of this erosion has been accentuated more in the East where the Turonian is no
389 longer continuous and appears in tatters. However in the margin of San Pedro, the Turonian is
390 not in flap but is continuous on the scale of the margin. The other identified reservoirs are not
391 continuous either because they are eroded or have not been deposited.

392 **➤ Petrophysical evaluation**

393
394 The petrophysical evaluation shows that the different reservoirs identified are of good quality
395 because their petrophysical characteristics are in line with those of a quality reservoir
396 according to [13]. However, the strong cementation of sandstone at some levels has
397 contributed to the reduction of porosity and has influenced overall petrophysical properties
398 that could have been better. [24] have shown that the porosity of rocks is related to the
399 diagenesis and the dissolution of certain minerals, the low porosity of the reservoirs of the
400 MSP2 well.

401 This study also shows that the study area was affected by transgressions and regressions that
402 caused lateral and vertical facies variations. These phenomena could sensibly modify the
403 petrophysical characteristics of the reservoirs.

404 **➤ Deposit environment**

405
406
407 Comparison of the Gamma Ray signatures of the reservoirs identified with the standard model
408 established by [9] shows that sedimentation of the study area started in a fluvial environment
409 and continued in a marine environment. The variations recorded in the different phases are
410 mainly due to the numerous transgressions and regressions movements experienced by the

411 Ivorian sedimentary basin. Indeed, [25] and [26] showed that the deep oceanic domain of the
412 Ivorian basin recorded three transgressive episodes.
413 It begins with the transgression of the Upper Albian, which is not a generalized phenomenon
414 at the scale of the whole basin [2]. At the end of the Upper Albian, there is a generalized
415 regression on the scale of the whole basin which marks the passage from the Albian to the
416 Cenomanian.
417 This regression, which marks the passage from the Albian to the Cenomanian, results in an
418 important discordance of the Cenomanian on the Albian.
419 The Cenomanian reservoirs (R1) would have deposited during this regression, or the littoral
420 conditions favorable to the deposition of fluvial types prevailed in the basin.
421 At the Cenomanian, there is a re-watering of the basin. This second transgressive episode
422 generalized throughout the basin will continue until the end of the Lower Senonian.
423 This marine transgression is highlighted in the MSP4 well where all the tanks have been
424 highlighted and deposited in a marine environment.
425 This marine transgression is interrupted at times by periods of regression, thus generating
426 fluvial and deltaic deposits observed in the Turonian reservoirs of the MSP1 and MSP3
427 wells.
428 According to [2], in the Lower Senonian, there is another regressive phase which causes a
429 strong erosion of the deposits of the Lower Senonian and in places those of the Turonian.
430 This regression is highlighted in this study by the deposition of deltaic or fluvial sediments
431 that cover the marine deposits in the MSP3 well.
432 This period is characterized by clay-sandstone deposits enriched locally in limestone.
433 The third transgressive episode occurs in the Upper Senonian.

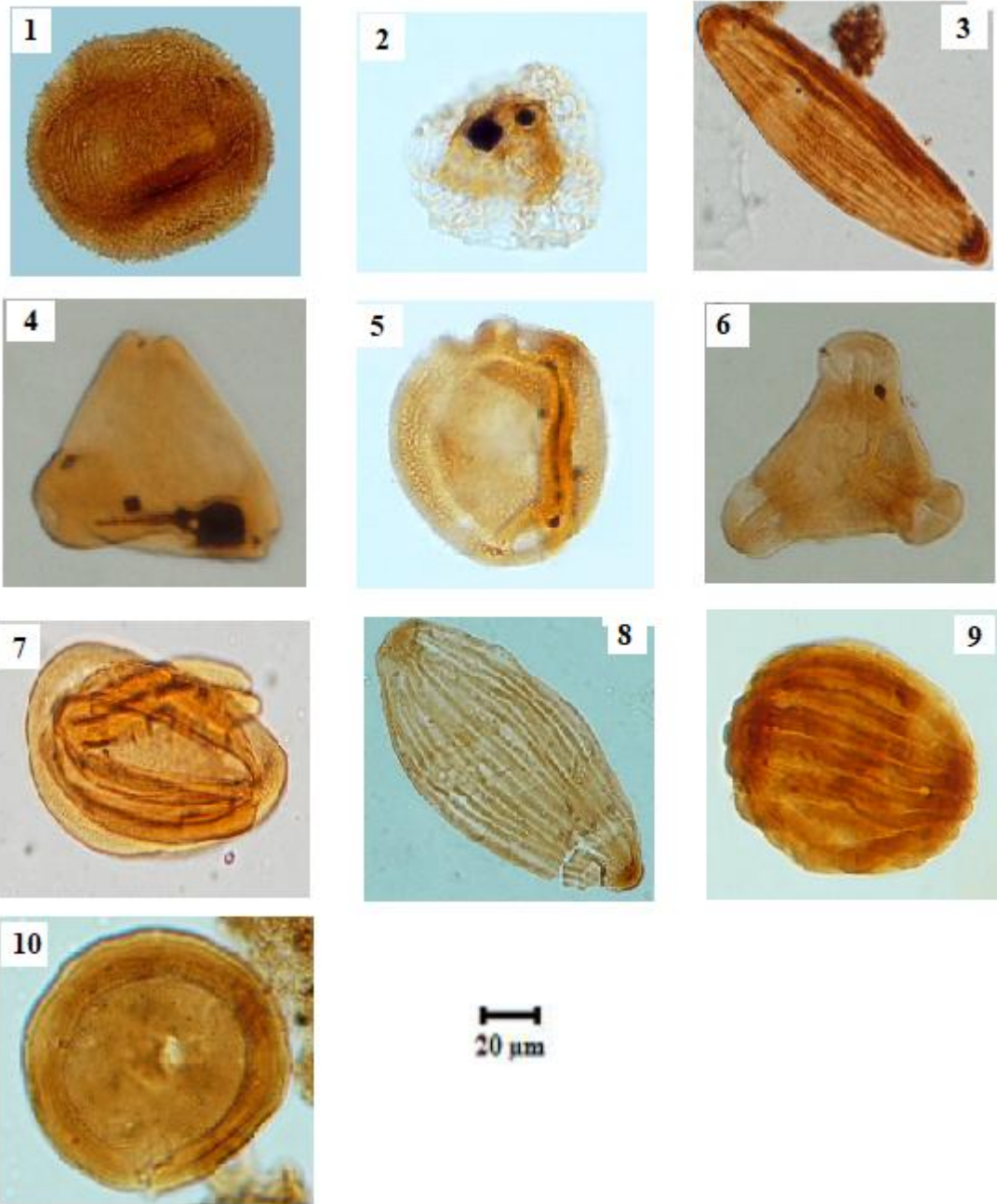
434 435 436 **6. CONCLUSION** 437

438 This study made it possible to characterize the Cenomanian, Turonian and Lower Senonian
439 reservoirs of four oil wells located on the margin of San Pedro.
440 On the lithostratigraphic level, the analysis of log log data and log gamma ray revealed a total
441 of ten (10) reservoir levels in all four wells studied in the Cenomanian-Santonian interval.
442 These reservoir levels identified, are mainly sandstone with fine grains and with limestone or
443 clay cement. These reservoir are surmounted by clay or silts that serve as rock cover.
444 **Lithological** synthesis has shown that these sandstones come from the mainland and are
445 deposited in a marine or deltaic environment with low to high energy.
446 Petrophysically, petrophysical parameters have shown that reservoirs are of good quality; they
447 have all the conditions necessary to store hydrocarbons. However, their high water saturation
448 makes them aquifers.
449

450
451
452
453
454
455
456

457 Plate 1: Cenomanian palynomorphs

458



459

460

461 1-*Classopolis echinatus*, 2-*Afropollis jardinus*, 3- *Stevesipollenites binodosus*, 4- *Triorites*
462 *africaensis*, 5- *Classopollis* sp.; 6- *Pemphixipollenites inequixinus*, 7- *Galeocornea causea*,
463 8- *Ephedripites* sp., 9- *Gnetaceapollenites diversus*, 10- *Classopollis classoides*.

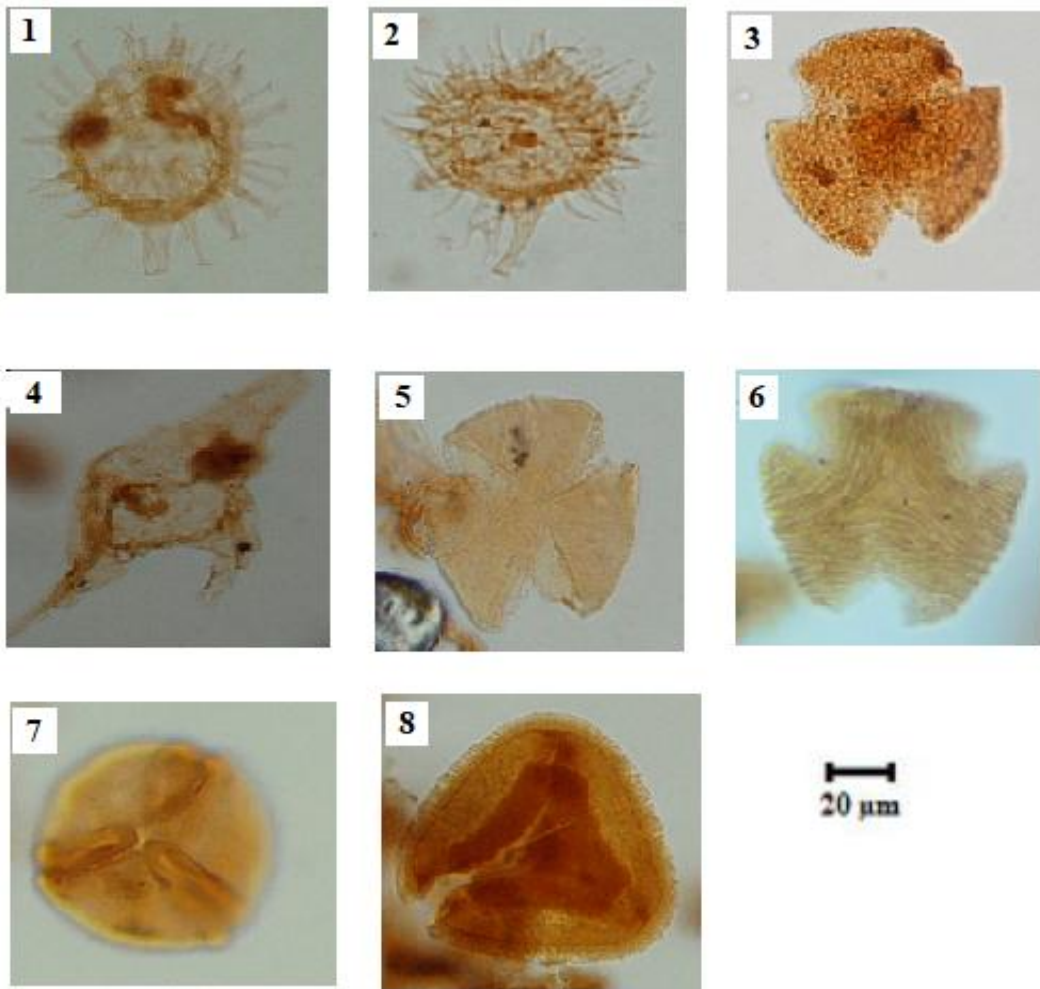
464

465

466

467

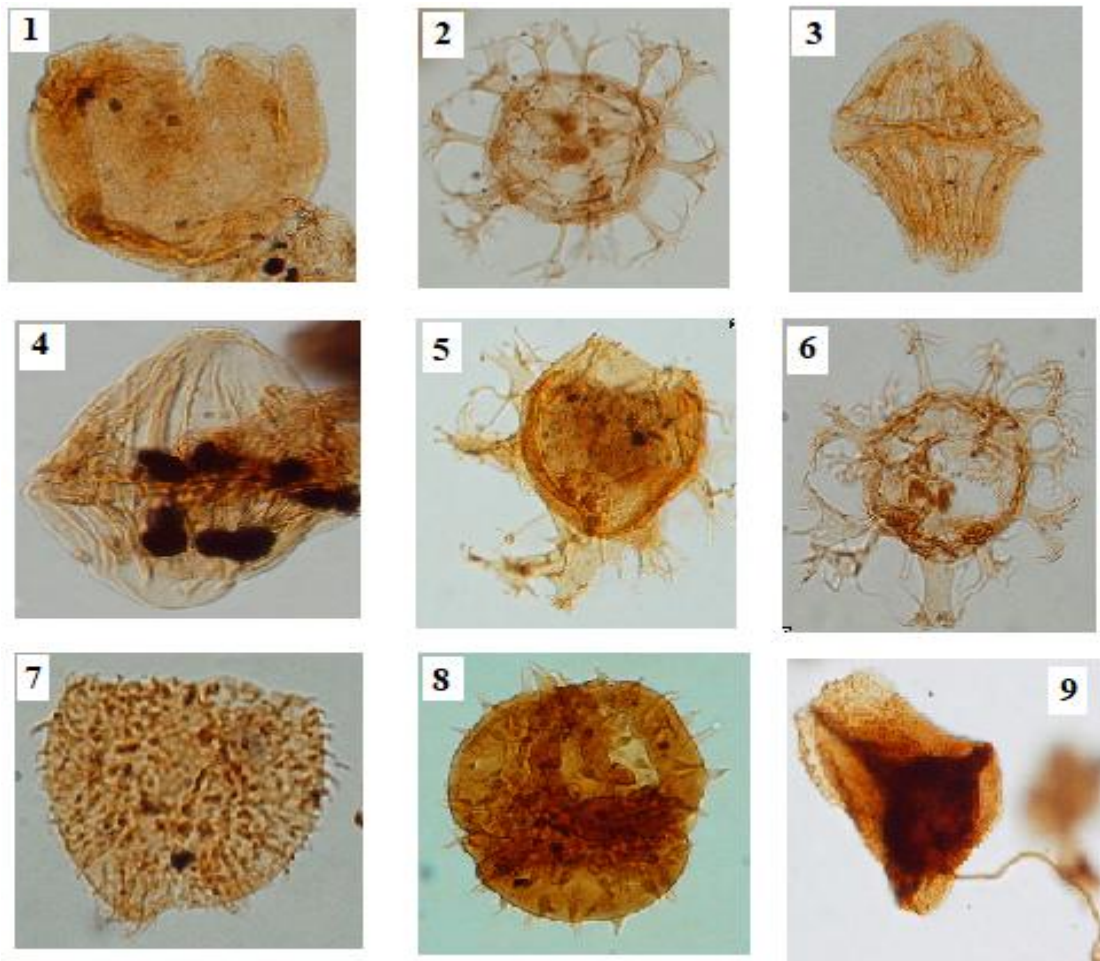
468 **Plate 2 : Turonian palynomorph**



469
470 1-*Florentinia radiculata*, 2- *Florentinia* sp., 3- *Tricolpites giganteus*, 4- *Odontochitina*
471 *operculata*, 5- *Tricolpites* sp., 6- *Tricolpites microstriatus*, 7- *Tricolpites* sp. SCI 348-155, 8-
472 *Parasyncolpites* sp.

473
474
475
476
477
478
479
480
481

482 **Plate 3 : Early Senonian Palynomorphs (Coniacian-Santonian)**



20 um

483

484

485 1- *Canningia* sp., 2- *Oligosphaeridium* complex, 3- *Dinogymnium acuminatum*, 4-
486 *Dinogymnium* sp., 5- *Xenascus* sp., 6- *Oligosphaeridium pulcherrinum*, 7- *Circulodinium*
487 *distinctum*, 8- *Droseridites senonicus*, 9- *Ariadnaesporites spinosus*.

488

489

490

491

492

493

494

495

496

497 **REFERENCES**

498

499 1. Goua TE. Biostratigraphy and palaeoenvironmental evolution of the Maastrichtian and
500 Paleocene series in the Ivorian coastal sedimentary basin. PhD Thesis, Univ. Burgundy,
501 Center for Earth Sciences. 1997; 354.

502

503 2. Sombo BC. Study of the structural and seismo-stratigraphic evolution of the offshore
504 sedimentary basin of Côte d'Ivoire, passive margin notched with a canyon. PhD thesis of
505 Earth Sciences. Univ. of Abidjan (Ivory Coast). 2002; 304.

506

507 3. Blarez E. The continental margin of Côte d'Ivoire-Ghana; structure and evolution of a
508 transforming continental margin. PhD Thesis, Univ. Paris VI (France). 1986; 188.

509

510 4. Mascle J, Blarez E. Evidence for transforming the evolution of the Ivory Coast-Ghana
511 Continental margin. Nature. 1986; 32: 378-381.

512

513 5. Digbehi ZB. Comparative study of early Atlantic opening stages: Gulf of Guinea and Bay
514 of Biscay (Sedimentology-Biostratigraphy). PhD thesis, University of Pau, (France). 1987;
515 366.

516

517 6. Basile C, Mascle J, Sage F, Lamarche G, Pontoise B. Precursor and site surveys: synthesis
518 of marine geological and geophysical data on the Ivory Coast-Ghana transform margin.
519 Tectonophysics. 1996; 159: 47-60.

520

521 7. Petroci. Côte d'Ivoire Petroleum evaluation. Internal report.1990 ; 99.

522

523 8. Delor C, Diaby I, Tastet JP, Yao B, Simeon Y, Vidal M, Dommanget A. Explanatory
524 notice of the geological map to 1/200 000, Sheet Abidjan, Mém. Dir. Geol., No. 3, Abidjan
525 (Ivory Coast). 1992a; 26.

526

527

528 9. Emery D, Myers KJ. "Sequence stratigraphy", Black Ltd., Oxford, U.K. 1996 ; 297.

529

530

531 10. Serra O. Delayed logging (basics of interpretation), Volume 1: Logging data acquisition,
532 Bull. Hundred. Rech. Explor. Prod. Elf Aquitaine. 1979 ; 625.

533

534 11. Timur A. "Pulsed nuclear magnetic resonance studies of porosity, movable fluid, and
535 permeability of sandstones. Journal of petroleum technology, US.1969 ;775-786.

536

537

538 12. Archie GE. The electrical Resistivity log as an aid in determining some reservoir
539 characteristics. Petroleum Transactions of the AIME. 1942 ; 54-62.

540

541

542 13. Monicard RP. Properties of reservoir rocks: Core analysis. French Institute of Petroleum
543 (Technip). 1980; 168.

544

545

- 546 14. Bamba KM, Digbehi ZB, Sombo CB, Goua TE, N'da LV. Planktonic foraminifera,
547 biostratigraphy and palaeoenvironment of Albo-Turonian deposits of Ivory Coast, West
548 Africa. *Journal of Paleobiology*. 2011; 30 (1): 1-11.
549
550
- 551 15. Jardine S, Magloire L. Palynology and stratigraphy of Cretaceous basins of Senegal and
552 Ivory Coast. *Same. Off. Rech. Geol. and Min.* 1965; 32: 187-245.
553
- 554 16. N'da LV, St. Mark P, De Klasz I, Goua TE. Micropaleontological data on the Cretaceous-
555 Tertiary passage of Ivory Coast. *Spanish review micropaleontologia*. 1995; 27 (3): 197-152.
556
- 557 17. Chierici MA. Stratigraphy, paleoenvironment and geological evolution of the Ivory Coast-
558 Ghana basin. In *geology of Africa and the South Atlantic. Proceedings of the conferences of*
559 *Angers, Mem. 16, Elf Aquitaine*. 1996; 293-303.
560
- 561 18. Digbehi ZB, N'da LV, Yao KR, Atteba YA. Principal Cretaceous foraminifers and
562 palynomorphs of the sedimentary basin of Ivory Coast, Gulf of Northern Guinea: proposals
563 for a local biostratigraphic scale. *Africa Geoscience Review*. 1997 ; 4 (3): 461-473.
564
- 565 19. Essay AA. Signature of gammas ray logging and deposit environments in A1 block, end
566 of study work, INP-HB. 2005; 63.
567
- 568 20. Kiki A, Kaki C, Almeida GA. Logging method evaluation of sandstone reservoir
569 characteristics of the Albian Formation in the deep offshore part of the Beninese coastal
570 basin. *Science of life, earth and agronomy*. 2018; 6: 15-22.
571
- 572 21. Petroci, Beicip. Ivory Coast Petroleum evaluation. Internal report. 2010; 130.
573
- 574 22. Bie G. Evolution of the microflora of the sedimentary basin of Côte d'Ivoire (Abidjan
575 margin) during the Cenozoic: palynostratigraphy, paleobotany, evolution of deposition
576 environments and maturation of organic matter. PhD thesis, Félix Houphouët Boigny
577 University, UFR of Earth Sciences and Mining Resources, (Abidjan, Ivory Coast). 2012; 245.
578
- 579 23. Spengler (A.), Delteil UR. The secondary-tertiary basin of Côte-d'Ivoire. In: *Symposium*
580 *on African Coastal Basins, New Delhi. ASGA, Paris*. 1966; 99-113.
581
- 582
- 583 24. Yao KC, Kouassi KA, Boga AH, World S, Digbehi ZB, N'da LV. Contribution to log
584 characterization of Cretaceous carbonate deposits in the sedimentary basin of Côte d'Ivoire
585 *European Scientific Journal*. 2016; 12: 394-410.
586
- 587 25. Petters SW. Paleoenvironment of the gulf of guinea *oceanologica Acta., SP Symposium*
588 *C3, Continental Geology of Margins. nineteen eighty one*. 1983; 81-85.
589
- 590 26. Mobio TM. Lithostratigraphic characterization of the Turonian of the eastern zone of the
591 offshore sedimentary basin of Côte d'Ivoire, DEA dissertation, marine geology, University of
592 Cocody, (Abidjan, Ivory Coast). 2007; 61.
593
594
595

596
597
598

UNDER PEER REVIEW